

## Dynamics of electrocorticographic (ECoG) activity in human temporal and frontal cortical areas during music listening

Cristhian Potes<sup>a,b,1</sup>, Aysegul Gunduz<sup>a,c,1</sup>, Peter Brunner<sup>a,c,d</sup>, Gerwin Schalk<sup>a,b,c,e,f,g,\*</sup>

<sup>a</sup> BCI R&D Program, Wadsworth Center, New York State Department of Health, Albany, NY, USA

<sup>b</sup> Department of Electrical and Computer Engineering, University of Texas at El Paso, TX, USA

<sup>c</sup> Department of Neurology, Albany Medical College, Albany, NY, USA

<sup>d</sup> Department of Computer Science, Graz University of Technology, Graz, Austria

<sup>e</sup> Department of Neurological Surgery, Washington University School of Medicine, St. Louis, MO, USA

<sup>f</sup> Department of Biomedical Engineering, Rensselaer Polytechnic Institute, Troy, NY, USA

<sup>g</sup> Department of Biomedical Science, School of Public Health, State University of New York at Albany, Albany, NY, USA

### ARTICLE INFO

#### Article history:

Accepted 7 April 2012

Available online 14 April 2012

#### Keywords:

Auditory processing

Electrocorticography (ECoG)

Sound intensity

High gamma activity

### ABSTRACT

Previous studies demonstrated that brain signals encode information about specific features of simple auditory stimuli or of general aspects of natural auditory stimuli. How brain signals represent the time course of specific features in natural auditory stimuli is not well understood. In this study, we show in eight human subjects that signals recorded from the surface of the brain (electrocorticography (ECoG)) encode information about the sound intensity of music. ECoG activity in the high gamma band recorded from the posterior part of the superior temporal gyrus as well as from an isolated area in the precentral gyrus was observed to be highly correlated with the sound intensity of music. These results not only confirm the role of auditory cortices in auditory processing but also point to an important role of premotor and motor cortices. They also encourage the use of ECoG activity to study more complex acoustic features of simple or natural auditory stimuli.

© 2012 Elsevier Inc. All rights reserved.

### Introduction

The neural substrates underlying the processing of complex sounds, such as voice or music, have not yet been fully elucidated (Griffiths and Warren, 2004; Kumar et al., 2007; Leaver and Rauschecker, 2010; Zatorre et al., 2004). Many studies on music perception and auditory processing have focused on the low-level acoustic features that compose complex sounds. For instance, loudness perception was found to be correlated to temporal acoustic features (e.g., sound intensity) within an auditory stream (Platel et al., 1997; Reiterer et al., 2008; Zatorre and Belin, 2001). Auditory processing of these acoustic features (i.e., sound intensity) has been extensively studied using functional magnetic resonance imaging (fMRI), positron emission tomography (PET), and scalp-recorded electroencephalography (EEG). These studies have identified cortical representations of sound intensity processing mainly in the primary and secondary auditory cortices (Jäncke et al., 1998; Langers et al., 2007; Mulert et al., 2005). fMRI (Jäncke et al., 1998; Langers et al., 2007) or combined fMRI/EEG studies (Mulert et al., 2005; Thaerig et al., 2008) found a linear relationship between blood flow or electrical activity in

the primary auditory cortex and sound intensity level. Other studies (Brechmann et al., 2002; Hart et al., 2003; Tanji et al., 2010; Yetkin et al., 2004) showed a relationship between sound intensity and the spatial extent of BOLD activations in the auditory cortex.

All these studies investigated brain responses to specific static features of simple auditory stimuli. Despite this body of work, it has been unclear to what extent brain signals encode dynamic acoustic features (such as the time course of sound intensity) in a continuous stream of music. Functional neuroimaging techniques (e.g., fMRI or PET) depend on metabolic processes (such as the hemodynamic response) and therefore measures signals that are produced by neuronal mass activity (Logothetis, 2008). These techniques cannot readily differentiate between different underlying physiological processes (such as local cortical processing vs. large-scale oscillatory activity) and have low temporal resolution (Aine, 1995; Shibasaki, 2008). On the other hand, EEG recordings provide electrophysiological measurements with high temporal resolution, but cannot capture local cortical processing that is reflected in high frequency field potentials, and also suffer from low spatial resolution (Nunez and Srinivasan, 2005). For instance, a recent EEG study by Schaefer et al. (2010) was able to differentiate seven different musical fragments based on single-trial event-related potentials. However, they could not accurately localize functionally significant areas due to the low spatial specificity of scalp recordings.

Electrocorticographic (ECoG) recordings from the surface of the brain combine high temporal resolution with relatively high spatial

\* Corresponding author at: Wadsworth Center, NYS Dept. of Health, C650 Empire State Plaza, Albany, NY 12201, USA.

E-mail addresses: [cmpotes@gmail.com](mailto:cmpotes@gmail.com) (C. Potes), [aysgunduz@gmail.com](mailto:aysgunduz@gmail.com) (A. Gunduz), [pbrunner@wadsworth.org](mailto:pbrunner@wadsworth.org) (P. Brunner), [schalk@wadsworth.org](mailto:schalk@wadsworth.org) (G. Schalk).

<sup>1</sup> Co-first authors.

resolution. ECoG activity in the high gamma range (i.e., ~70–170 Hz) is generally regarded as an accurate indicator of local cortical processing. For example, ECoG has been found to reflect higher-order auditory processing (Boatman-Reich et al., 2010; Crone et al., 2001; Edwards et al., 2005, 2009; Sinai et al., 2009) and aspects of speech or auditory perception (Crone et al., 2001; Edwards et al., 2009; Lachaux et al., 2007; Pasley et al., 2012; Ray et al., 2003; Sinai et al., 2009). Nevertheless, which ECoG features and locations encode dynamic aspects of acoustic features in continuous music has remained unknown.

The goal of this study was to determine the ECoG features and the cortical regions that are related to sound intensity of continuous music. Our results from 8 human subjects demonstrate for the first time that ECoG high gamma activity recorded from auditory and premotor and motor cortices accurately reflect the time course of the music's sound intensity.

## Materials and methods

### Subjects and data collection

The subjects in this study were eight patients with intractable epilepsy (4 women and 4 men) who underwent temporary implantation of subdural electrode arrays for the purpose of localization of seizure foci prior to surgical resection. Table 1 summarizes the subjects' clinical profiles. All of the subjects gave informed consent to participate in the study, which was approved by the Institutional Review Board of Albany Medical College. Preoperative Wada testing (Wada and Rassmussen, 1960) determined language lateralization to the left hemisphere in subjects A, B, C, D, E, and G; and bilateral language dominance in subject F. Language lateralization was not determined for subject H. None of the subjects had a history of hearing impairment. The implanted electrode grids (Ad-Tech Medical Corp., Racine, WI) consisted of platinum-iridium electrodes that were 4 mm in diameter (2.3 mm exposed), embedded in silicon, and were spaced with an inter-electrode distance of 1 cm. (The temporal lobe grid of subject F had electrodes with a 6 mm

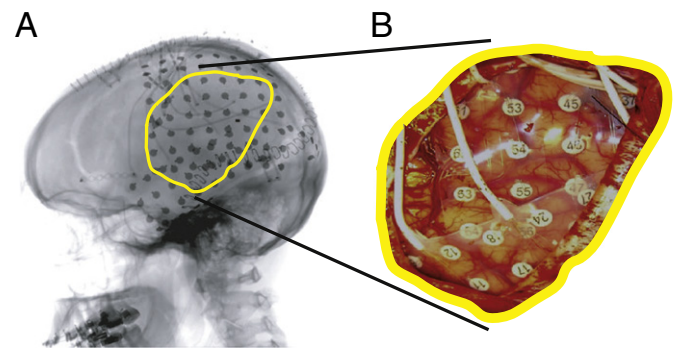


**Fig. 1.** Example of an implanted subdural grid in Subject B. (A) Lateral radiograph indicating grid position. (B) Subdural grid placed over left fronto-parietal and temporal lobes.

inter-electrode distance.) The total numbers of implanted electrodes were 99, 96, 83, 109, 58, 120, 58, and 59 for subjects A to H, respectively. Grid placement and duration of ECoG monitoring were based solely on the requirements of the clinical evaluation without any consideration of this study. Each subject had postoperative anterior–posterior and lateral radiographs, as well as computer tomography (CT) scans to verify grid locations (see Fig. 1).

The subjects were instructed to listen attentively to the song “Another Brick in the Wall – Part 1” (Pink Floyd, Columbia Records, 1979) while ECoG activity was recorded using the general-purpose software BCI2000 (Schalk and Mellinger, 2010; Schalk et al., 2004) that was connected to eight g.USBamp biosignal acquisition devices (g.tec, Graz, Austria). The song was 3:10 min long, digitized at 44.1 kHz in waveform audio file format, and binaurally presented to each subject using in-ear monitoring earphones (12 to 23.5 kHz audio bandwidth, 20 dB isolation from environmental noise). The sound volume was adjusted to a comfortable level for each subject.

ECoG signals were referenced to an electrocorticographically silent electrode (i.e., a location that was not identified as eloquent cortex by electrocortical stimulation mapping), digitized at 1200 Hz, synchronized with stimulus presentation, and stored with BCI2000. The recordings were visually inspected offline for environmental artifacts and interictal activity. Channels that did not clearly contain ECoG signals were removed from further analyses, which left 97, 86, 82, 104, 56, 108, 57, and 53 channels for subjects A to H, respectively.

### Cortical mapping

We used Curry software (Neuroscan Inc., El Paso, TX) to create subject-specific 3D cortical brain models from high-resolution pre-operative magnetic resonance imaging (MRI) scans. We co-registered the MRIs with post-operative computer tomography (CT) images and extracted, for each grid electrode, the stereotactic coordinates and functional area according to the Talairach Atlas (Lancaster et al., 2000). We used the 3D cortical template provided by the Montreal Neurological Institute (MNI)<sup>2</sup> for cross-subject analysis and for subject A, whose brain model was not available. Finally, we projected the electrodes onto the subject-specific brain models shown in Fig. 2 to render activation maps using custom MATLAB software.

### Extraction of ECoG features

We were interested in the spectral amplitudes of the ECoG signals in the mu (8–12 Hz), beta (18–24 Hz), low gamma (35–45 Hz) and high gamma (70–170 Hz) bands because these frequency bands have been shown in previous ECoG studies to be task-related (e.g., motor movement Miller et al., 2007; Schalk et al., 2007), speech production (Pei et

**Table 1**

Clinical profiles of the subjects that participated in the study. All of the subjects had normal cognitive capacity and were functionally independent. Language lateralization (LL) was based on the Wada test.

Subject	Age	Sex	Handedness	LL	Seizure focus	Grid locations	# of elec.
A	24	M	R	L	Right temporal	Right fronto-parietal	64
B	29	F	R	L	Left temporal	Left fronto-parietal	35
C	30	M	R	L	Left temporal	Left temporal pole	23
D	26	F	R	L	Left temporal	Left occipital	3
E	45	M	R	L	Left temporal	Left frontal	6
F	29	F	R	Bilateral	Left temporal	Left temporal	40
G	45	F	L	L	Left temporal	Left temporal pole	35
H	60	M	R	NA	Left temporal	Left temporal pole	4
					Left occipital	Left occipital	6
					Left temporal	Left temporal	64
					Left temporal	Left temporal pole	35
					Left temporal	Left temporal pole	4
					Left temporal	Left occipital	4
					Left temporal	Left temporal	54
					Left temporal	fronto-temporal	4
					Left temporal	Left temporal pole	4
					Left temporal	Left temporal	40
					Left temporal	Left temporal pole	68
					Left temporal	Left temporal pole	4
					Left temporal	Left orbital pole	4
					Left temporal	Left occipital	4
					Left temporal	Left frontal	31
					Left temporal	Left temporal	27
					Left temporal	Left temporal	17
					Left temporal	Left	42
					Left temporal	parieto-occipital	

<sup>2</sup> <http://www.bic.mni.mcgill.ca>.

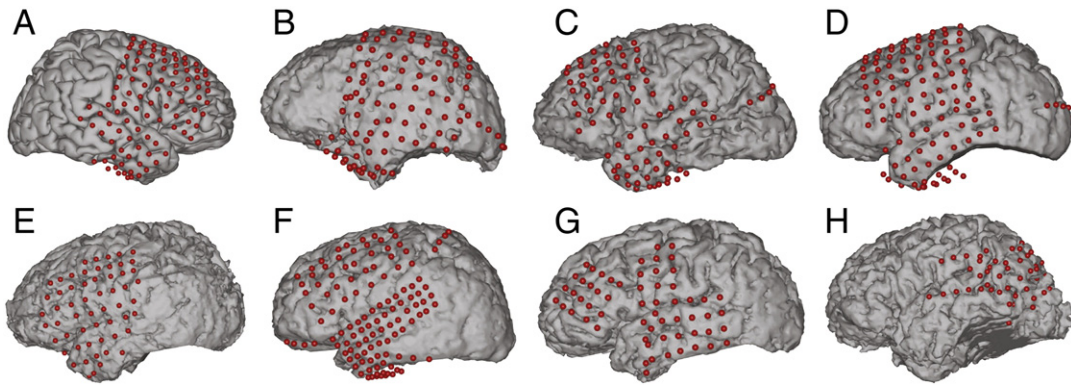


**Fig. 2.** Subject-specific brain models and projected electrode locations for subjects A to H. (The MNI brain was used for subject A because his brain model was not available.)

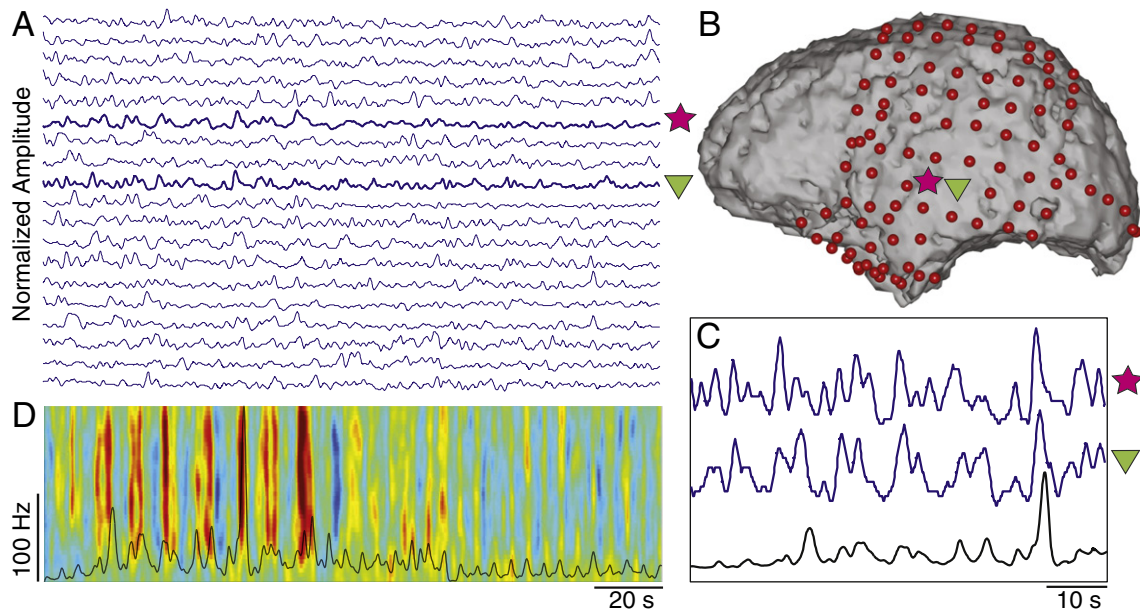


**Fig. 3.** Example of ECoG activity and its relationship with sound intensity in subject B. A: Time course of normalized high gamma amplitudes (blue traces) extracted from channels located in the left temporal lobe. B: Locations that exhibit a time course that is correlated with sound intensity are indicated with colored symbols and are shown on the subject's brain model. C: Magnification of time course of sound intensity (black trace) and high gamma of the indicated locations (blue traces). D: Time–frequency representation of the ECoG signal recorded from the cortical location indicated by the star symbol in B. The time course of sound intensity is shown in black.

al., 2011), or auditory processing (Pasley et al., 2012; Sinai et al., 2009). To extract these amplitudes, we first removed all frequencies below 0.1 Hz from the ECoG signals using a high-pass filter. A common average reference (CAR) spatial filter then removed spatial noise common to all ECoG channels. ECoG signals from each channel were band pass filtered at mu, beta, low gamma, and high gamma frequency bands (i.e., ECoG features). Next, we computed the magnitude of each of these ECoG features, followed by a low pass filter at 0.5 Hz. Similar results were obtained when using a low pass filter with different cut-off frequencies (e.g., 1 Hz and 3 Hz). Finally, ECoG signals in each band were downsampled to 10 Hz.

#### Extraction of sound intensity

We approached the analysis of the ECoG correlates of the song by studying its relationship with the song's sound intensity. To do this, we calculated the sound intensity as the average power derived from non-overlapping 10 ms segments of the song. Sound intensity was smoothed by applying a low pass filter at 0.5 Hz and then downsampled to 10 Hz. Fig. 3 shows an example of the time course of ECoG high gamma activity in temporal cortex derived from subject B and illustrates its relation to the time course of sound intensity. This figure

also illustrates a time–frequency representation of the ECoG signal recorded from the superior temporal gyrus.

## Results

### Relevant cortical locations

We first determined the cortical locations and frequency bands (i.e., the ECoG features) that were related to sound intensity. To do this, we calculated the pairwise Spearman's correlation<sup>3</sup> coefficient ( $r$ ) and its significance (i.e.,  $p$ -value) between sound intensity and each of the different ECoG features at each location. The resulted correlation coefficient ( $r$ ) has a  $t$ -distribution with  $df = 1798$  degrees of freedom. For those locations with significant correlation coefficients (i.e.,  $r > 0.3$  and  $p$ -value  $< 0.01$  after Bonferroni correction), we projected the negative logarithm of the corresponding  $p$ -values (i.e.,  $-\log_{10}(p)$ ) onto the corresponding individual brain model.<sup>4</sup> The negative logarithm of the

<sup>3</sup> We used Spearman's (non-parametric) correlation method rather than Pearson's (parametric) correlation, because it is less sensitive to outliers in the data.

<sup>4</sup> Note that a  $-\log_{10}(p)$  of 2 and higher is statistically significant at a confidence level of 99% (i.e.,  $p < 0.01$ ).

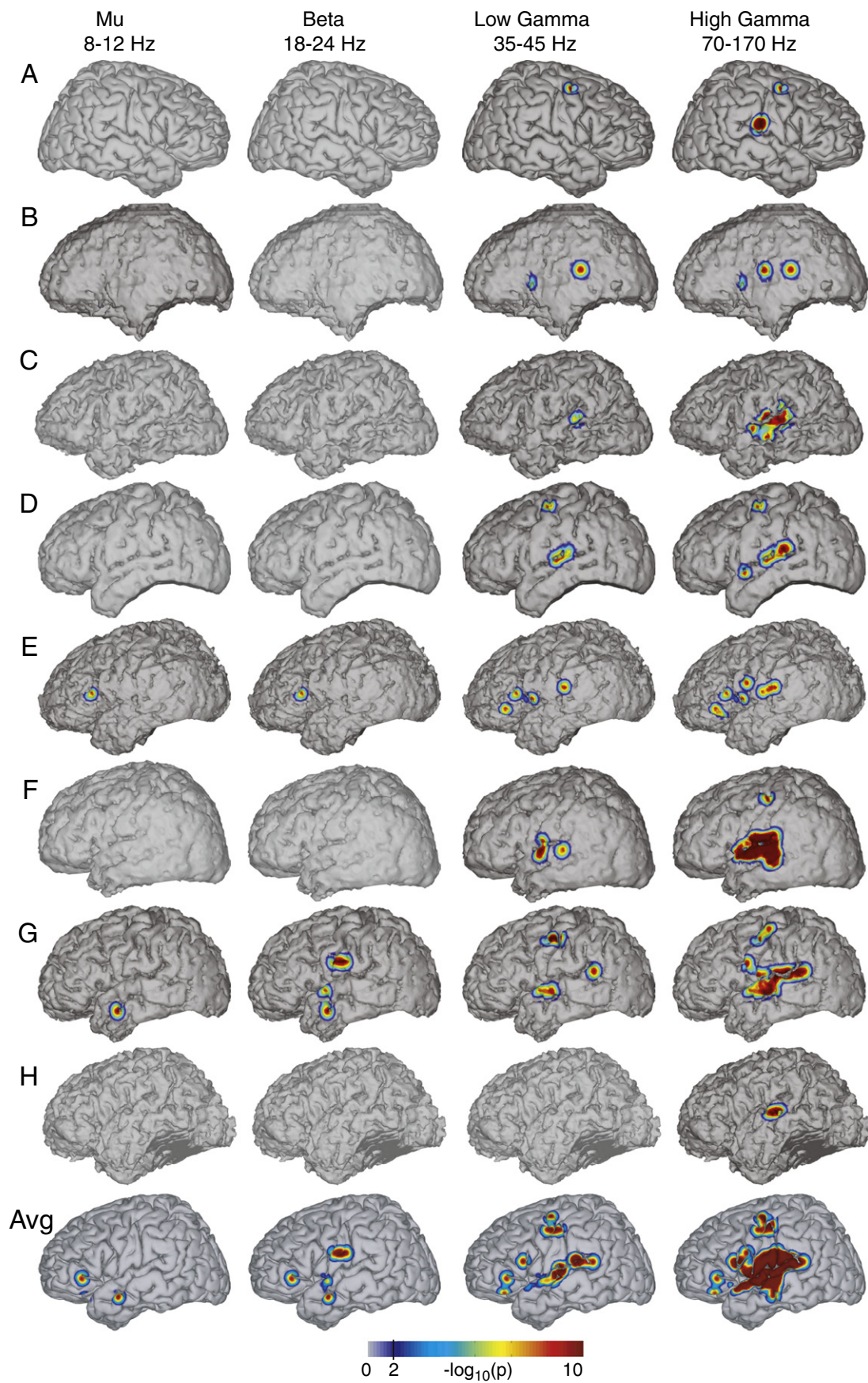


**Table 2**

Correlation coefficients computed between sound intensity and different ECoG features: mu (8–12 Hz), beta (18–24 Hz), low gamma (35–45 Hz), and high gamma (70–170 Hz) located over the posterior part of the superior temporal gyrus. These results demonstrate that high gamma activity yields the highest correlation in all subjects.

ECoG feature/subject	A	B	C	D	E	F	G	H	Avg
Mu	−0.14	0.1	−0.17	0.02	−0.04	−0.32	−0.4	−0.23	−0.15
Beta	−0.13	0.16	−0.03	0.11	0.11	−0.11	−0.33	−0.1	−0.04
Low gamma	0.16	0.37	0.31	0.22	0.31	0.11	0.30	0.02	0.23
High gamma	0.43	0.53	0.45	0.52	0.50	0.43	0.51	0.58	0.49

$p$ -value has been used in several previous studies (Gunduz et al., 2011; Kubánek et al., 2009; Schalk et al., 2007) to visualize results from similar correlation analyses. This metric is additive, so it can be used to show average brain activation across multiple subjects. The resulting topographies are shown in Fig. 4 for each subject and ECoG feature. These topographies show that high gamma band activations in or close to the superior temporal gyrus and precentral gyrus are significantly correlated with sound intensity. Similar topographies were obtained when we applied a low pass filter with different cut-off frequencies (e.g., 1 Hz and 3 Hz) to each ECoG feature and sound intensity as described in *Extraction of ECoG features* and *Extraction of sound intensity* sections.

From all these cortical locations, we then identified those locations in the superior temporal gyrus and precentral gyrus that had the highest correlation coefficients between ECoG high gamma and sound intensity, resulting in two identified locations for each subject. (Only subjects A, D, F, and G had locations with significant correlation coefficients in precentral gyrus.) Across all subjects, these locations were tightly clustered in the posterior part of the superior temporal gyrus and the dorsal part of the precentral gyrus, respectively. Table 2 shows for all subjects the correlation coefficients between each ECoG feature (mu, beta, low gamma, and high gamma) and sound intensity for the superior temporal gyrus locations. Figs. 5 and 6 show these cortical locations in superior temporal gyrus and precentral gyrus, respectively, as well as the time course of sound intensity and ECoG high gamma at the respective location. Our results confirm the importance of these areas for auditory processing found in previous neuroimaging studies (Brechmann et al., 2002; Chen et al., 2009; Griffiths and Warren, 2002; Hart et al., 2003; Jäncke et al., 1998; Langers et al., 2007; Popescu et al., 2004; Yetkin et al., 2004; Zatorre et al., 2007), an ECoG study (Edwards et al., 2010), and EEG studies (Mulert et al., 2005).

We then averaged ECoG high gamma activity for all these locations and for all subjects with grids implanted in the left hemisphere, separately for superior temporal gyrus and precentral gyrus, and correlated these two time series at different time lags. The maximum correlation coefficient  $r=0.70$  was obtained at lag  $\tau=110$  ms, which suggests that ECoG high gamma activity in auditory cortex precedes ECoG high gamma activity in premotor/motor cortex by 110 ms (Fig. 7).

Finally, Fig. 8 shows the spatial relationship of the location identified in precentral gyrus with locations classified as hand or face motor cortex using electrical stimulation mapping and/or passive functional ECoG mapping (Brunner et al., 2009). The location that was found to be related to auditory stimulation in this present study was different from hand or face motor locations in all subjects.

## Discussion

### *The role of ECoG gamma activity in sound processing*

This study shows for the first time that the time course of high gamma ECoG activity is highly correlated to the sound intensity of a continuous stream of music. While neural activity correlated to sound

intensity was mostly identified in the superior temporal gyrus, an additional isolated area in the precentral gyrus also showed a relationship with sound intensity in subjects A, D, F, and G. (It is quite possible that the absence of this location in the other subjects can be attributed to the limited spatial resolution of our recordings.) This area was not classified as hand or face motor cortex using electrical stimulation mapping or passive real-time ECoG mapping in any of these four subjects. This suggests then that the corresponding location is in fact related to a distinct aspect of auditory processing rather than to somatosensory or motor processing. However, future research is needed to determine the specific functional relevance of activations in the precentral gyrus such as rhythm processing (Zatorre et al., 2007) or speech processing (Edwards et al., 2010).

The average gamma activity in the superior temporal gyrus was highly correlated ( $r=0.70$ ) with the average gamma activity from the precentral gyrus, and was leading it by 110 ms. These results might be explained by previous findings in fMRI studies (Chen et al., 2009; Griffiths and Warren, 2002; Popescu et al., 2004; Zatorre et al., 2007) where they suggest that the posterior part of the superior temporal gyrus might act as a neural hub decomposing the various types of sound and integrating those of motor relevance with the prefrontal, premotor, and motor regions through a dorsal pathway. Our results also support the hypothesis that activity in the high gamma band, in contrast to activity at lower frequencies, co-localize with hemodynamic responses measured with fMRI during sound intensity processing (Hermes et al., in press; Jäncke et al., 1998; Lachaux et al., 2007; Langers et al., 2007; Logothetis et al., 2001). Although the neurophysiological origin of high gamma activity in ECoG is still a matter of some debate, recent research supports the hypothesis that it is a reflection of the mean firing rate of the neuronal population directly beneath the electrode contact (Manning et al., 2009; Müller, 2010). The concurrence of our results with fMRI studies in humans and single-unit studies in primates, and ECoG's high temporal and relatively high spatial resolutions, strongly encourage further study of high gamma ECoG activity and its relationship to other acoustic features.

### *Current experimental limitations*

The present results are encouraging, and could not have readily been derived using other imaging techniques. At the same time, there will ultimately be limits to what can be achieved using the currently used subject population. Our study, like practically all human ECoG studies to date, relied on electrode grids implanted for clinical reasons. Thus, grid coverage is incomplete and variable across subjects. Given the limited number of subjects with grids implanted over the right (1 subject) and left (7 subjects) brain hemispheres, further research is needed to determine potential hemispheric differences during music processing. The physical and cognitive conditions and level of cooperation of each patient are impaired and/or variable. In addition, auditory stimulation was not highly controlled during the experiment. This relatively uncontrolled experimental situation is in contrast to typical

**Fig. 4.** Significance of cortical areas for sound intensity processing. This figure shows the spatial distribution of  $-\log_{10}(p)$  values obtained from the (univariate) correlation between sound intensity and each ECoG feature. The last row corresponds to the average spatial distribution of  $-\log_{10}(p)$  values for subjects with electrode grids implanted only in the left brain hemisphere (i.e., subjects B to H). Values larger than 2 are statistically significant at a confidence level of 99% (see vertical line in color bar). High gamma activations are focused mainly over the superior temporal gyrus and precentral gyrus.

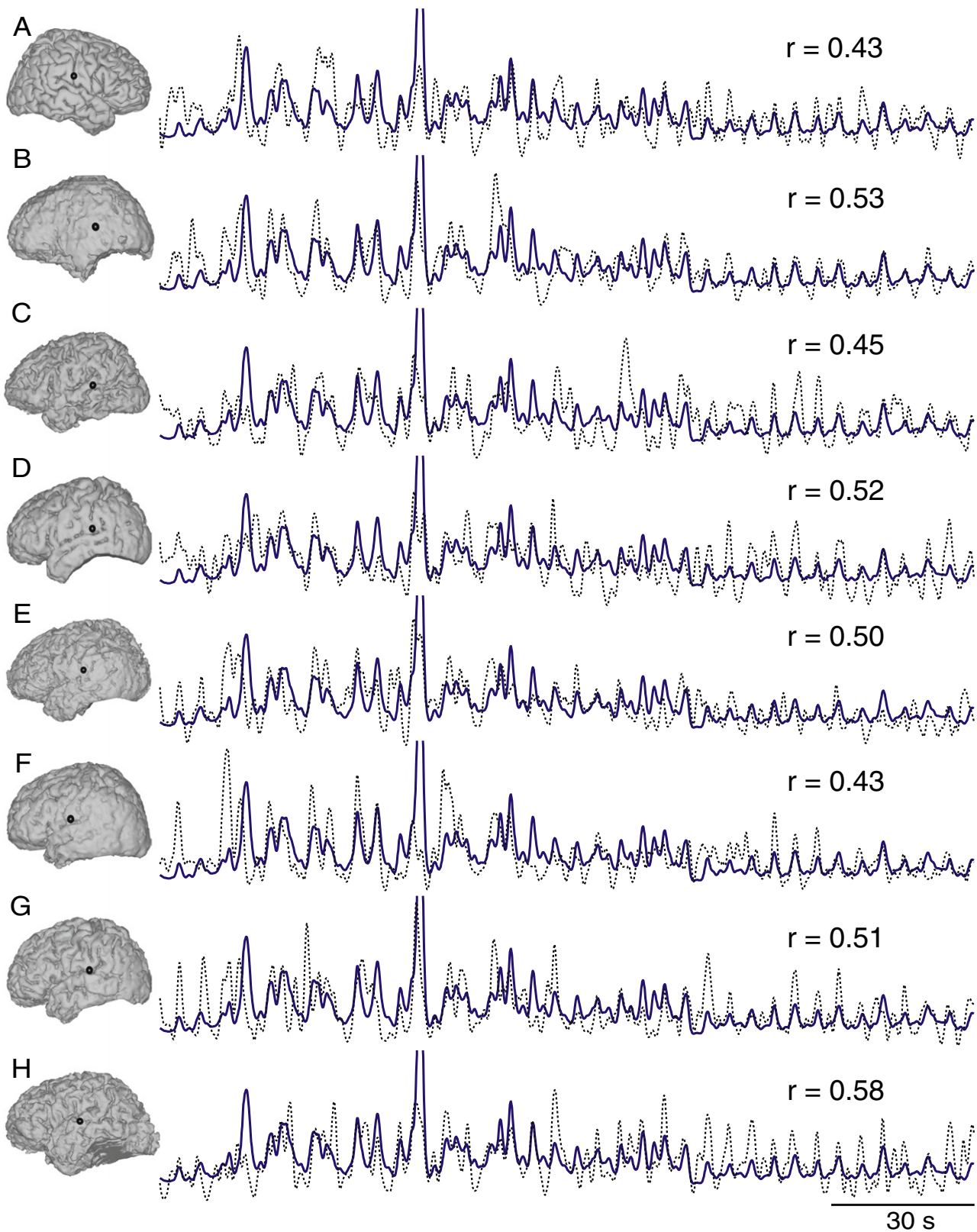


**Fig. 5.** Cortical locations (black dots) in the posterior part of the superior temporal gyrus with the highest correlation between ECoG high gamma (dashed black trace) and sound intensity (blue trace). The respective correlation coefficients,  $r$ , for each subject are also given.

neuroscientific studies, in which experimental conditions are usually highly controlled. Finally, the subjects in the study are epileptic patients, and thus may have some degree of functional reorganization compared

to healthy individuals. Variability in the correlation values at the same cortical locations across subjects might be explained by variances introduced by different sources such as grid coverage, physical and cognitive

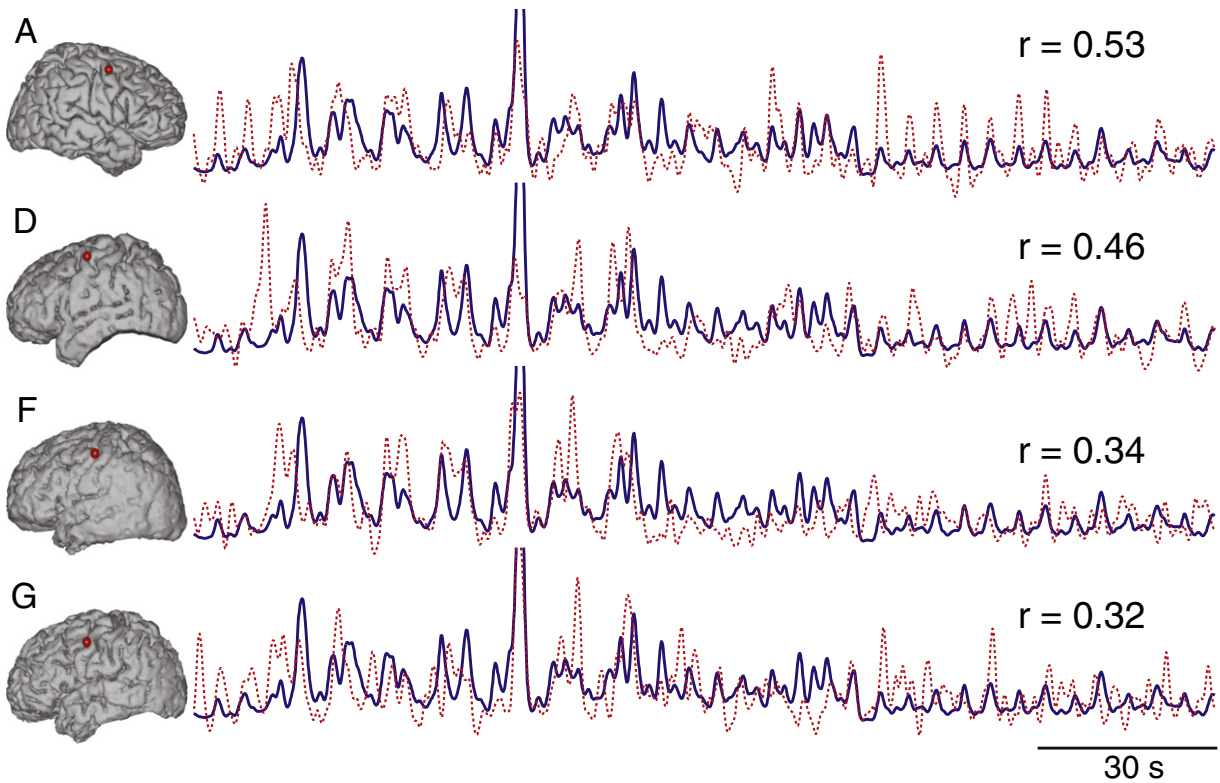


**Fig. 6.** Cortical locations (red dots) in the dorsal part of the precentral gyrus with the highest correlation between ECoG high gamma (dashed red trace) and sound intensity (blue trace). (Only subjects A, D, F, and G had locations with significant correlation coefficients.) The respective correlation coefficients,  $r$ , for each subject are also given.

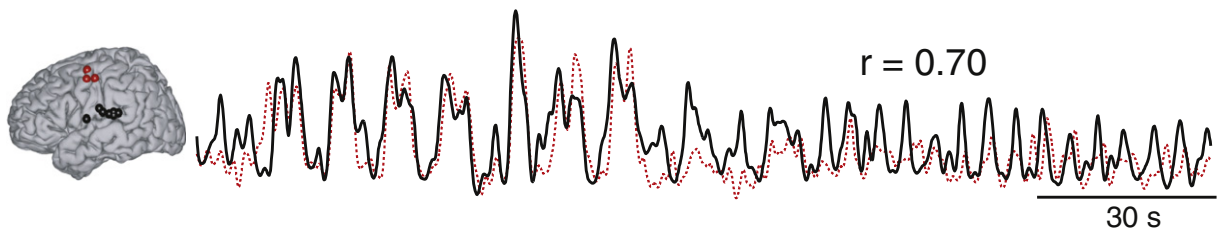


**Fig. 7.** Left: locations in the superior temporal gyrus and precentral gyrus identified in Figs. 5 and 6. Right: average time course of ECoG high gamma for these locations in the superior temporal gyrus (black trace) and the precentral gyrus (dashed red trace). Subject A who has grid implanted in the right brain hemisphere was not considered to compute the average. The corresponding correlation coefficient,  $r$ , is also given.

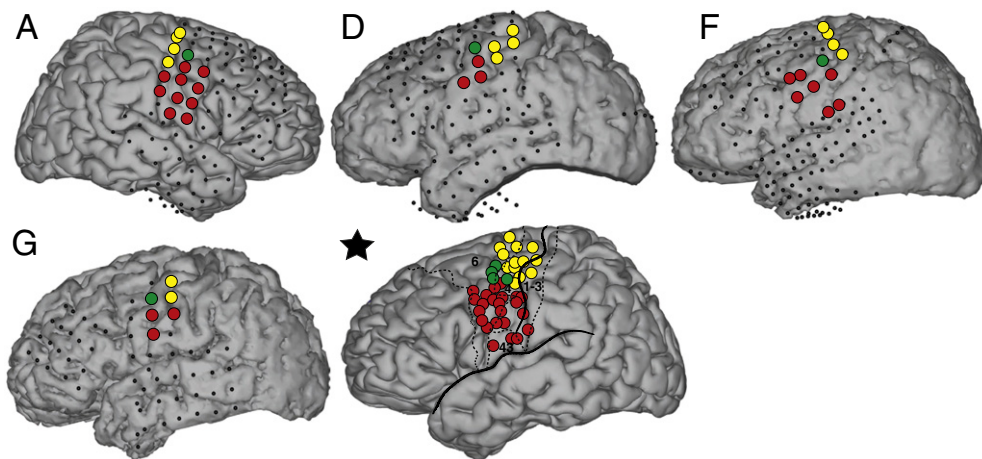


**Fig. 8.** Cortical mapping of face (red circles) and hand (yellow circles) motor areas identified using electrocortical stimulation mapping and/or real-time passive ECoG mapping (Brunner et al., 2009). Coverage of all other electrodes is shown using small black dots. Electrodes in green are the same locations from subjects A, D, F, and G shown in Fig. 6. The brain figure marked with a star shows the MNI brain, the locations of all highlighted electrodes for subjects A, D, F, and G, as well as relevant cortical landmarks.

conditions, and the subject's specific neuroanatomy. Despite these issues, the results presented in this and other ECoG studies are usually consistent with expectations based on the neuroanatomy or on results from other imaging modalities.

While the subjects had a broad spatial coverage, including coverage of the temporal lobe, the analytical detail of our results is limited in spatial resolution by the inter-electrode distance (0.6–1 cm) of the implanted grids. Grid electrodes with smaller contacts and inter-electrode distances have recently been implanted and used to study language processing (Kellis et al., 2009; Wilson et al., 2006). Increased resolution of the ECoG grids will likely improve further and refine our understanding of underlying ECoG physiology.

The placement of the electrode grids in this study was based on the clinical needs of the patients for the localization of epileptic foci, which typically originate from a single hemisphere. Hence, we could not investigate brain lateralization of acoustic processing as suggested in Belin et al. (1998); Gourévitch et al. (2008); Platel et al. (1997); Zatorre and Belin (2001). For instance, these studies demonstrated specialization of the right hemisphere for fine spectral changes such as the pitch. Comprehensive access to both hemispheres, which will likely remain impractical, would allow for a more complete analysis of auditory processing.

#### Future work

Our study demonstrated the relationship of ECoG features with sound intensity in a continuous stream of music. Future work may investigate the relationship between ECoG features and other aspects of sounds or their perception, such as loudness perception. Loudness perception is a subjective measure that cannot be universally measured by a single metric and can be affected by several acoustic parameters such as sound intensity, bandwidth, and duration. Decoding of perceived loudness from brain signals may have important applications for the calibration of stimulation levels of cochlear implants. Currently, these levels are adjusted by an audiologist and have to be frequently reprogrammed due to implant scar formation or habituation.

#### Acknowledgments

The authors would like to thank Dr. Disha Gupta for her comments and assistance with data recording. This work was supported by grants from the US Army Research Office (W911NF-07-1-0415, W911NF-08-1-0216) and the NIH/NIBIB (EB006356 and EB000856).

#### References

Aine, C.J., 1995. Crit. Rev. Neurobiol. 9 (2–3), 229–309.  
 Belin, P., McAdams, S., Smith, B., Savel, S., Thivard, L., Samson, S., Samson, Y., 1998. J. Neurosci. 18 (16), 6388–6394.  
 Boatman-Reich, D., Franaszczuk, P.J., Korzeniewska, A., Caffo, B., Ritzl, E.K., Colwell, S., Crone, N.E., 2010. Front. Comput. Neurosci. 4, 4.  
 Brechmann, A., Baumgart, F., Scheich, H., 2002. J. Neurophysiol. 87 (1), 423–433.  
 Brunner, P., Ritaccio, A.L., Lynch, T.M., Emrich, J.F., Wilson, J.A., Williams, J.C., Aarnoutse, E.J., Ramsey, N.F., Leuthardt, E.C., Bischof, H., Schalk, G., 2009. Epilepsy Behav. 15, 278–286.  
 Chen, J.L., Penhune, V.B., Zatorre, R.J., 2009. Ann. N. Y. Acad. Sci. 1169, 15–34.  
 Crone, N.E., Boatman, D., Gordon, B., Hao, L., 2001. Clin. Neurophysiol. 112 (4), 565–582.  
 Edwards, E., Soltani, M., Deouell, L.Y., Berger, M.S., Knight, R.T., 2005. J. Neurophysiol. 94 (6), 4269–4280.

Edwards, E., Soltani, M., Kim, W., Dalal, S.S., Nagarajan, S.S., Berger, M.S., Knight, R.T., 2009. J. Neurophysiol. 102 (1), 377–386.  
 Edwards, E., Nagarajan, S., Dalal, S., Canolty, R., Kirsch, H., Barbaro, N., Knight, R., 2010. Neuroimage 50 (1), 291–301.  
 Gourévitch, B., Le Bouquin Jeannès, R., Faucon, G., Liégeois-Chauvel, C., 2008. Hear. Res. 237 (1–2), 1–18.  
 Griffiths, T.D., Warren, J.D., 2002. Trends Neurosci. 27 (7), 348–353.  
 Griffiths, T.D., Warren, J.D., 2004. Nat. Rev. Neurosci. 5 (11), 887–892.  
 Gunduz, A., Brunner, P., Daitch, A., Leuthardt, E., Ritaccio, A., Pesaran, B., Schalk, G., 2011. Front. Hum. Neurosci. 5, 1–11.  
 Hart, H.C., Hall, D.A., Palmer, A.R., 2003. Hear. Res. 179 (1–2), 104–112.  
 Hermes, D., Miller, K.J., Vansteensel, M.J., Aarnoutse, E.J., Leijten, F.S.S., Ramsey, N.F., in press. Hum. Brain Mapp. <http://dx.doi.org/10.1038/mp.2011.188>.  
 Jäncke, L., Shah, N.J., Posse, S., Grosse-Ryken, M., Müller-Gärtner, H.W., 1998. Neuropsychologia 36 (9), 875–883.  
 Kellis, S.S., House, P.A., Thomson, K.E., Brown, R., Greger, B., 2009. Neurosurg. Focus 27 (1), E9.  
 Kubánek, J., Miller, K.J., Ojemann, J.G., Wolpaw, J.R., Schalk, G., 2009. J. Neural Eng. 6 (6), 066001.  
 Kumar, S., Stephan, K.E., Warren, J.D., Friston, K.J., Griffiths, T.D., 2007. PLoS Comput. Biol. 3 (6), e100.  
 Lachaux, J.P., Fonlupt, P., Kahane, P., Minotti, L., Hoffmann, D., Bertrand, O., Bacia, M., 2007. Hum. Brain Mapp. 28 (12), 1368–1375.  
 Lancaster, J.L., Woldorff, M.G., Parsons, L.M., Liotti, M., Freitas, C.S., Rainey, L., Kochunov, P.V., Nickerson, D., Mikiten, S.A., Fox, P.T., 2000. Hum. Brain Mapp. 10 (3), 120–131.  
 Langers, D.R.M., van Dijk, P., Schoenmaker, E.S., Backes, W.H., 2007. Neuroimage 35 (2), 709–718.  
 Leaver, A.M., Rauschecker, J.P., 2010. J. Neurosci. 30 (22), 7604–7612.  
 Logothetis, N.K., 2008. Nature 453 (7197), 869–878 URL: <http://dx.doi.org/10.1038/nature06976>.  
 Logothetis, N.K., Pauls, J., Augath, M., Trinath, T., Oeltermann, A., 2001. Nature 412 (6843), 150–157.  
 Manning, J.R., Jacobs, J., Fried, I., Kahana, M.J., 2009. J. Neurosci. 29 (43), 13613–13620.  
 Miller, K.J., 2010. J. Neurosci. 30 (19), 6477–6479.  
 Miller, K., Leuthardt, E., Schalk, G., Rao, R., Anderson, N., Moran, D., Miller, J., Ojemann, J., 2007. J. Neurosci. 27 (9), 2424.  
 Muler, C., Jäger, L., Propp, S., Karch, S., Störmann, S., Pogarell, O., Möller, H., Juckel, G., Hegerl, U., 2005. Neuroimage 28 (1), 49–58.  
 Nunez, P.L., Srinivasan, R., 2005. Electric Fields of the Brain: The Neurophysics of EEG. Oxford University Press.  
 Pasley, B.N., David, S.V., Mesgarani, N., Flinker, A., Shamma, S.A., Crone, N.E., Knight, R.T., Chang, E.F., 2012. PLoS Biol. 10 (1), e1001251.  
 Pei, X., Barbour, D., Leuthardt, E., Schalk, G., 2011. J. Neural Eng. 8, 046028.  
 Platel, H., Price, C., Baron, J.C., Wise, R., Lambert, J., Frackowiak, R.S., Lechevalier, B., Eustache, F., 1997. Brain 120 (Pt. 2), 229–243.  
 Popescu, M., Otsuka, A., Ioannides, A., 2004. Neuroimage 21 (4), 1622–1638.  
 Ray, S., Jouny, C.C., Crone, N.E., Boatman, D., Thakor, N.V., Franaszczuk, P.J., 2003. IEEE Trans. Biomed. Eng. 50 (12), 1371–1373.  
 Reiterer, S., Erb, M., Grodd, W., Wildgruber, D., 2008. Brain Imaging and Behav. 2 (1), 1–10.  
 Schaefer, R.S., Farquhar, J., Blokland, Y., Sadakata, M., Desain, P., 2010. Neuroimage 56 (2), 843–849.  
 Schalk, G., Mellinger, J., 2010. A Practical Guide to Brain–Computer Interfacing with BCI2000, 1st edn. Springer, London, UK.  
 Schalk, G., McFarland, D.J., Hinterberger, T., Birbaumer, N., Wolpaw, J.R., 2004. IEEE Trans. Biomed. Eng. 51 (6), 1034–1043.  
 Schalk, G., Kubánek, J., Miller, K.J., Anderson, N.R., Leuthardt, E.C., Ojemann, J.G., Limbrick, D., Moran, D., Gerhardt, L.A., Wolpaw, J.R., 2007. J. Neural Eng. 4, 264–275.  
 Shibasaki, H., 2008. Clin. Neurophysiol. 119 (4), 731–743.  
 Sinai, A., Crone, N.E., Wied, H.M., Franaszczuk, P.J., Miglioretti, D., Boatman-Reich, D., 2009. Clin. Neurophysiol. 120 (1), 140–149.  
 Tanji, K., Leopold, D.A., Ye, F.Q., Zhu, C., Malloy, M., Saunders, R.C., Mishkin, M., 2010. Neuroimage 49 (1), 150–157.  
 Thaerig, S., Behne, N., Schadow, J., Lenz, D., Scheich, H., Brechmann, A., Herrmann, C.S., 2008. Int. J. Psychophysiol. 67 (3), 235–241.  
 Wada, J., Rassmussen, T., 1960. Neurosurgery 17, 266–282.  
 Wilson, J.A., Feltton, E.A., Garell, P.C., Schalk, G., Williams, J.C., 2006. IEEE Trans. Neural Syst. Rehabil. Eng. 14 (2), 246–250.  
 Yetkin, F.Z., Roland, P.S., Christensen, W.F., Purdy, P.D., 2004. Laryngoscope 114 (3), 512–518.  
 Zatorre, R.J., Belin, P., 2001. Cereb. Cortex 10, 946–953.  
 Zatorre, R.J., Bouffard, M., Belin, P., 2004. J. Neurosci. 24 (14), 3637–3642.  
 Zatorre, R.J., Chen, J.L., Penhune, V.B., 2007. Nat. Rev. Neurosci. 8, 547–558.